

Nationaal Lucht- en Ruimtevaartlaboratorium

National Aerospace Laboratory NLR



NLR-TP-98184

GEROS: a European grid generator for rotorcraft simulation methods

M.H.L. Hounjet

C.B. Allen

L. Gasparini, L. Vigevano

A. Pagano



NLR-TP-98184

GEROS: a European grid generator for rotorcraft simulation methods

M.H.L. Hounjet

C.B. Allen*

L. Gasparini** , L. Vigevano**

A. Pagano***

* *University of Bristol*

** *Politecnico di Milano (PMI)*

*** *Centro Italiano Ricerche Aerospaziali S.C.p.A. (CIRA)*

This investigation has been carried out under a contract awarded by the European Commission, contract number BRPR-CT96-0162, and partly as a part of NLR's basic research programme, Working Plan number A.1.C.2.

This report is based on a presentation to be held on the 6th International Conference on Numerical Grid Generation in Computational Field Simulation, 6-9 July 1998, University of Greenwich, London, England.

The contents of this report may be cited on condition that full credit is given to NLR and the authors.

Division: Fluid Dynamics
Issued: May 1998
Classification of title: unclassified

Summary

A grid generator system for the modelling of complex multi-bladed rotors is under development in Europe as a part of the development of a complete rotorcraft simulation method: The Brite/EuRam EROS project. The grid generator [1] exploits a CHIMERA domain decomposition on structured grids. The development is being carried out by rotorcraft manufacturers (Agusta, ECD, GKN-Westland), research centres (CIRA, DERA, DLR, NLR, ONERA), and Universities (Polit. Milano, Univ. Bristol, Univ. Glasgow, Univ. Rome 3). It addresses the industrial need for a rotor aerodynamic prediction tool [2] able to capture rotational phenomena, such as blade tip and wake vortices, and to predict correctly the unsteady blade pressures over a range of flight conditions, from hover to high-speed forward flight. This paper presents and discusses the capabilities of the GEROS grid generator together with relevant results.

Keywords Grid generation, Chimera, rotorcraft

Contents

1	Introduction	5
2	General features of GEROS code	7
3	Modelling	8
3.1	Grid topologies	8
3.2	Surface grid generation	8
3.3	Volume grid generation	9
3.4	Volume grid quality assessment and improvements	9
3.5	Volume grid dynamics	10
3.6	Adaptation	10
3.7	CHIMERA tagging and interpolation	10
4	Applications	12
5	Conclusion	13
6	Acknowledgements	14
7	References	15

13 Figures

(29 pages in total)

1 Introduction

In the development of modern rotorcraft, unsteady aerodynamic analysis is required in a large design space. This implies the development of computer methods to determine the unsteady flow about realistic rotorcraft configurations which have to be executed efficiently on suitable computational grids. Typically the rotor flies in its own wake of shed/trailed vorticity, and experiences very large rates of dynamic changes in geometry as well as flow (shock-induced separation, dynamic stall, shock waves). The problem poses specific requirements to the grids and the grid generating procedures. The multiple bodies in relative motion (fuselage, main and tail rotor blades, platform) with strong elastic deformations are ideal for application of multiple grids. Even isolated rotor calculations require grids with varying characteristics to capture accurately the wakes, the shocks and to cluster the points along characteristic surfaces at an intermediate distance from the blade where adequate resolution is needed to obtain useful data for acoustic prediction codes. The adequate capturing of the helicoidal rotor wakes over large distances places unique requirements on maintaining quality of the grids in the far field. Also for hover simulations the front and aft boundaries are required to form a perfect match at the inter-blade plane to avoid interpolation errors. Single-block grids are limited to simple bladeshapes and are inefficient for accurately capturing/adapting the vorticity regions. Computational grids may be generated with existing 'universal' grid generation methods such as the multi-block methods and unstructured grid methods, at the expense however of a few drawbacks: 1) multi-block methods are too demanding for 'non-grid expert' applicators and 2) multi-block and unstructured grids increase the computation time and the development time considerably. The last category is, furthermore, considered not mature enough for a complete rotor simulation in forward flight. A key problem is that since the geometric modelling is hard to decouple, none of the existing packages covers fully the dynamic geometrical problems that need to be addressed: surface grid generation, volume grid generation, volume grid adaptation/ deformation/ rotation/ positioning, dynamic connectivity and animation/prototyping of the dynamic geometries. The latter requires resort to external software and external specialists which often cannot be secured.

The EROS consortium has decided to develop a CHIMERA¹ [3] type grid generator for application to complete rotorcraft, aiming at solving the aforementioned problems. The grid generator has been designed in particular to generate grids of acceptable quality about advanced rotorcraft blades for the modelling of:

- 1 multiblade calculations in hover with wake capturing;

¹multiblock grids might be considered as a particular case of the CHIMERA approach

2 multiblade calculations in forward flight with wake modelling (grid generated around a single blade) and with wake capturing (grid generated around the full rotor);

with and without elastic deformations, and should be easy to use for 'non-grid expert' applicators and cover all aspects mentioned above.

The CHIMERA approach is selected for its natural adaptation to flow and dynamic (static) geometry characteristics (complexities), reduced wall clock times by simplifying grid generation, better accuracy using shape conforming grids and short familiarization times. The approach has been applied to rotorcraft already by many researchers [4-8].

The often repeated drawbacks of the CHIMERA approach, namely that defects in conservation of flow fluxes might lead to impaired solutions, is considered to be of minor importance as other sources of uncertainty coming from the geometrical state description of the structure (hinge angles, mass and stiffness) are larger. Add to this also that the quality of the grids might have a similar impact [9]. Also the setting up of the connectivity (which is approximately $O(N^{\frac{2}{3}})$, N is number of vertices) is supposed to be a smaller task compared with generating the connectivity involved in unstructured methods. The latter need dynamic adaptation to resolve the flow gradient properly and have to upgrade the connectivity for a major part of the flow domain ($O(N)$).

At present the basic components of the method have been realized and research is being directed at improving the critical components in the process cycle.

The paper presents the past development and status of the GEROS gridgenerator and shows relevant results.

2 General features of GEROS code

This chapter summarizes the features of the GEROS method. GEROS exploits the CHIMERA domain decomposition on structured grids and approaches an **ALL-in-ONE** capability for grid generation by providing the following key features:

- Surface grid generation
- Volume grid dynamics (deformation and motion)
- Volume grid quality analysis
- Volume grid CHIMERA tagger (connectivity arranger)
- Interactive control with on-line help functionality
- Script driven batch operations
- Volume grid generation
- Volume grid aposteriori quality enhancement
- Volume grid elliptic smoothing
- Visual inspection and prototyping
- Coded in FORTRAN77 with FORTRAN90 extentions.
- Script control

The embedded script facility allows the gridding process to be repeatable and to be documented. It is also helpful when adaptation is required for the surface grids in which case a new surface grid can be generated based on the original input data by a reversed call of the solver. The prototyping feature allows the inspection and animation of the location and other characteristics of the deforming grids and their connectivity in relative motion for all azimuthal angles and blades prior to the CFD simulation. The main structure of the GEROS code which is divided into 6 subsystems to perform the aforementioned main tasks is depicted in figure 1. ¹

The modelling applied in the submodules is explained in the next chapter.

¹The VISUAL3 [10] library is used for plotting.

3 Modelling

This chapter describes the characteristics of models/features embedded in the GEROS code.

3.1 Grid topologies

The following topologies are provided:

- **single-block meshes:** Helicopter rotor simulations (with and without prescribed wake geometry) with CFD methods are usually performed on the basis of single-block structured meshes. The choice of the most suitable grid topology is more critical due to the fact that it is impossible to satisfy the requirements with respect to resolution in the flow domain with a realistic number of mesh points.
- **Periodic blade: CC, CH, OC and OH** The considered physical domain has a cylindrical shape, parallel to the rotor axis, covering the whole rotor disk or an azimuthal sector of it. For hover simulations only an angular sector of the rotor plane containing one blade is accounted for. To avoid interpolation errors the distribution of grid points at the front and the rear boundary is constrained so as to achieve a perfect match between both (periodicity) planes, thus avoiding the need for interpolation.
- **Non-periodic blade: CC, CH, OC and OH**
- **Cap: HO** So-called cap grids are developed for dealing with the tip region and tip vortex.
- **Collar: OH** A so-called collar grid topology (*OH*) is developed for dealing with the hub region and the main blade.
- **Background:HH and OH** Cartesian background and cylindrical background grids are developed for dealing with the flow about one chord length away from the blades.
- **Tip-vortex:HH and OH** Cartesian and cylindrical grids are developed for dealing with the flow centred at the tip-vortex position.

The O grids are preferred here to reduce the overlap zones as much as possible and to obtain a uniform spacing in the overlap zones.

3.2 Surface grid generation

Surface grid generation is the obvious basis for the volume grid generation method. The surface grid on the body is generated from the interpolation of discrete inputs of coordinates. These inputs might be obtained as output from most CAD/CAM packages or from a set of blade sections, and are organized as a network of geometrical patches linked by a connection table. The surface grid generation is performed also for the elements of such a network: a set of patch surface

grids whose edges have a unique connection or are free. This network architecture allows a very flexible specification of the grid spacing in different portions of the geometrical body. A mono-block structured surface description and/or panelling of the body parts is then generated by interpolating¹ and assembling the separate parent surface grids.

3.3 Volume grid generation

Taking into account the fact that due to the CHIMERA approach the geometric complexities are very much reduced, the development has been restricted to a relatively simple algebraic grid [14] generator. Hyperbolic methods [11] which generate high-quality grids for complex geometries and for viscous grids and hardly need user interaction, are not considered as they are more elaborate to code, hard to control in the far field and need ad-hoc modifications at apices.

The formulation of the algebraic grid generation method is as follows:

$$\vec{r}_{i j k} = \psi_1^0(k)\vec{r}_{i j k=0} + \psi_1^1(k)\vec{n}_{i j} + \psi_2^0(k) \left[\psi_2^0(k)\vec{r}_{i j nk} + \psi_1^0(k)\vec{r}_{i j nk+1} \right]. \quad (1)$$

The aforementioned equations constitute a 4-variables interpolation scheme using one free parameter to control spacing and stretching and is being based on: $\vec{r}_{i j k=0}$, the grid point at the body(slit); $\vec{n}_{i j}$, the normal at the body(slit). $\vec{r}_{i j k=nk}$, the corresponding grid point at the far field boundary; $\vec{r}_{i j k=nk+1}$, a regularized grid point in the far field and; the set of blending functions which depend on the stretching parameter st : $\zeta = \frac{k}{nk}$, $\bar{\zeta} = \left\{ \frac{e^\zeta - 1 - \zeta}{e - 2} \right\}^{st}$, $\psi_1^0 = 1 - \bar{\zeta}$, $\psi_1^1 = \sqrt{\bar{\zeta}} - \left\{ \frac{e^{\bar{\zeta}} - 1 - \bar{\zeta}}{e - 2} \right\}$, $\psi_2^0 = \bar{\zeta}$.

For the non-boundary conforming HH Cartesian or cylindrical grids spacing control is exercised with the hyperbolic distributions.

3.4 Volume grid quality assessment and improvements

The accuracy of a numerical solution of a flow simulation and the stability of the flow solver are obviously connected to some characteristic measures of the grid. The following local and global measures are defined for a grid: i) cross-over and negative cell volumes; ii) orthogonality (skewness); iii) smoothness and iv) aspect ratio. These indicators may help in defining some empirical criteria, which a grid has to satisfy to allow for stable and accurate flow calculations. The quality can be improved by post application of an elliptical smoother [12]. Furthermore an a posteriori procedure [13] is developed to improve the algebraic grids (eliminate cross-over and

¹bilinear and NURBS

negative cell volumes, increase orthogonality and smoothness, and obtain uniform cell volumes).

The quality measures are also used in defining the priority in the CHIMERA tagging.²

3.5 Volume grid dynamics

The geometric state of the grids is dynamically changing according to:

- rigid motions of the whole rotorcraft
- rigid rotations of the whole blade assembly about the main rotor axis.
- rigid rotations of the individual blades about the hinges (flapping, pitching and lagging)
- rigid motion of the tip-vortex capture grids.
- elastic deformations of the individual blades.

The rigid motions do not require a change of the relative position of points in the same grids. For grid deformation the transfinite algebraic method [14] is applied. Because the grid deformation of the child grids is usually in normal direction this method is expected to be satisfactory.

3.6 Adaptation

For reasons of efficiency and accuracy the grids should be adapted to account for improved capturing of the shock waves and the vortical flowfields. Instead of developing feedback procedures (redistribution, source control terms) to create a grid more consistent with the observed physical phenomena preference is given to explicit adaptation strategies which fits naturally in the CHIMERA approach. Therefore adaptation will be applied by opting for special adaptation grids (agents).³ These are dedicated high resolution thin-layer grids near the bodies which will only be active (dominant) in zones where high gradients occur. Outside the thin-layer the adaptation is performed by uniform Cartesian grids.⁴

3.7 CHIMERA tagging and interpolation

The connectivity between the grids is dynamic and requires a continuous upgrading in the case of forward flight where changes might occur at each time step. The developed algorithm is similar to the CMPGRD algorithm [15] which has a clear modular structure, and places almost no restrictions on the layout of the child grids and easily allows for future improvements. At present a hierarchical grid arrangement is preferred for reasons of efficiency. For the cases to be dealt within the EROS project it is required that, except for the background grid, each of the embedded

²In progress

³In progress

⁴Direct dynamic adaptation at each timestep is considered inappropriate for non-periodic time-accurate flows.



grids is fully embedded with respect to the one that envelops it. Work is in progress to improve the algorithm by using the quality measures in discriminating between fringes and support grids and the connectivity obtained at previous timesteps. The most time-consuming component in terms of efficiency is the methodology for identifying the holes. The current method employs an analytical method whenever possible, a bounding box and a stencil walk concept and uses ideas explained in [16]. In the future tree-like accelerations [17] might be adopted.

It is acknowledged that higher order interpolation leads to non-monotonic results and trilinear interpolation is applied within a hexahedral support box. This requires a reverse mapping of the support box utilizing a Newton procedure for identifying the local coordinates of the fringe point in a hexahedron. Work is in progress to improve upon this situation by the application of so-called volume spline methods [18]. The latter are expected to have advantages of higher spatial accuracy without wiggles and do not require a reverse mapping. They operate in Cartesian coordinates therefore reducing the work needed in identification.

4 Applications

At present the system is nearly complete and first results are available. An application to a BERP rotor blade is presented in figures 2-10. Figure 2 shows the surface grid of the base geometry. The other figures show a periodic OH topology type volume grid about the blade together with embedded HH topology type grids¹ for capturing the tip vortices of the current blade and the preceding one. The volume grids (Figs. 3,4 and 6) have been smoothed elliptically. Figs. 9 and 10 show typical sceneries during the animation of a grid setup (background + OH grid) for a 4-bladed pitching/flapping rotor.

The stages of advancement applied in the tagging options are demonstrated in figs. 11-13 for a two-element airfoil: trivial tagging which results in a maximum overlap (fig. 11); CMPGRD type tagging in which the child has the priority (fig. 12) and; *smart* tagging² in which the smallest volumes have priority (fig. 13);. The last case is clearly the better.

¹helicoidals with rectangular cross-section

²In progress

5 Conclusion

The first version of a common European grid generator code for the modelling of complex multi-bladed rotors has been presented. It is an essential part of the development of a complete rotorcraft simulation method: The Brite/EuRam EROS project.

Relevant results of the grid generator exploiting a CHIMERA domain decomposition on structured grids have been presented.

6 Acknowledgements

The authors would also like to thank A. D'Alascio and P. Renzoni (CIRA) , S.P. Fiddes (University of Bristol) and A. Kokkalis (WESTLAND) for their contributions to the development.

7 References

1. Hounjet, M.H.L., D'Alascio, A., Renzoni, P., Pahlke, K., Westland, J., Gasparini, L., Vigevano, L., Allen, C.B., Fiddes, S.P., Dubuc, L., and Kokkalis, A., *A Formulation of a Grid Generator for a Rotorcraft Simulation Method*, NLR TR 97024 L, January 1997.
2. D'Alascio, A., Renzoni, P., Hounjet, M.H.L., van der Vegt, J.J.W., Boniface, J.-C., Sidès, J., Gasparini, L., Vigevano, L., Allen, C.B., Dubuc, L., Salvatore, F., Morino, L., and Schöll, E., *Formulation of an Euler Rotorcraft Simulation Method*, CIRA-TR-97-044, April 1997.
3. J.A. Benek, P.G. Buning and J.L. Steger *A 3-D Chimera grid embedding method*, AIAA-85-1523.
4. R.L. Meakin, *Moving body overset grid methods for complete aircraft tiltrotor simulations*, AIAA-93-3550
5. K. Pahlke and J. Raddatz, *Flexibility enhancement of Euler codes for rotor flows by chimera techniques.*, In *Proceedings of the 20th European Rotorcraft Forum*, Amsterdam, (NL), October 1994.
6. R. Stangl and S. Wagner, *Calculation of steady rotor flow using an overlapping-embedded grid technique.*, In *Proceedings of the 18th European Rotorcraft Forum*, Avignon, France, September 1992.
7. E.P.N. Duque and G.R. Srinivasan, *Numerical Simulation of a Hovering Rotor Using Embedded Grids*, In *Proceedings of the 48th Annual American Helicopter Society Forum*, Washington, D.C., June 1992.
8. J. Ahmad and E.P.N. Duque, *Helicopter rotor blade computation in unsteady flows using moving overset grids.*, AIAA Journal of Aircraft, 33(1):54–60, January-February 1996.
9. R.L. Meakin, *On the spatial and temporal accuracy of overset grid methods for moving body problems*, AIAA-94-1925-CP
10. Haimes, R., *VISUAL3 Users & Programmers Manual*, MIT
11. M.H.L. Hounjet, *Hyperbolic grid generation control by panel methods*. NLR-TP 91061-U, NLR, 1991.
12. J.F. Thompson, *A general three-dimensional elliptic grid generation system on a composite block-structure*, Computer Methods in applied Mechanics and Engineering, Vol.64, pp 377-411, 1987
13. B.W. Siebert and G.S. Dulikravich, *Grid generation using a posteriori optimization with geometrically normalized functionals*, AIAA-90-3048
14. C.B. Allen, *Grid Adaptation for Unsteady Flow Computations*, Proceedings I.Mech.E. Journal of Aero. Eng., Vol 211, Part G, 1997.

15. G. Chesshire, W.D. Henshaw, *Composite Overlapping Meshes for the Solution of Partial Differential Equations*, J. C. Phy., 90, pp 1-64, 1990.
16. W.F. LaBozzetta, T.D. Gatzke, S. Ellison, G.P. Finfrock, and M.S. Fisher. *MACGS-Towards the complete grid generation system*. AIAA-94-1923-CP, 1994.
17. N.A. Peters, *Hole Cutting for 3-D overlapping grids*. CHA/NAV/R-97/0052 (Submitted to SIAM J. Sci. Comp.)
18. M.H.L. Hounjet and J.J. Meijer ,*Evaluation of Elastomechanical and Aerodynamic Data Transfer Methods for Non-planar Configurations in Computational Aeroelastic Analysis* ,in Proc. of CEAS Int. Forum on Aeroelasticity and Structural Dynamics , 1995, pp. 11.1-11.24

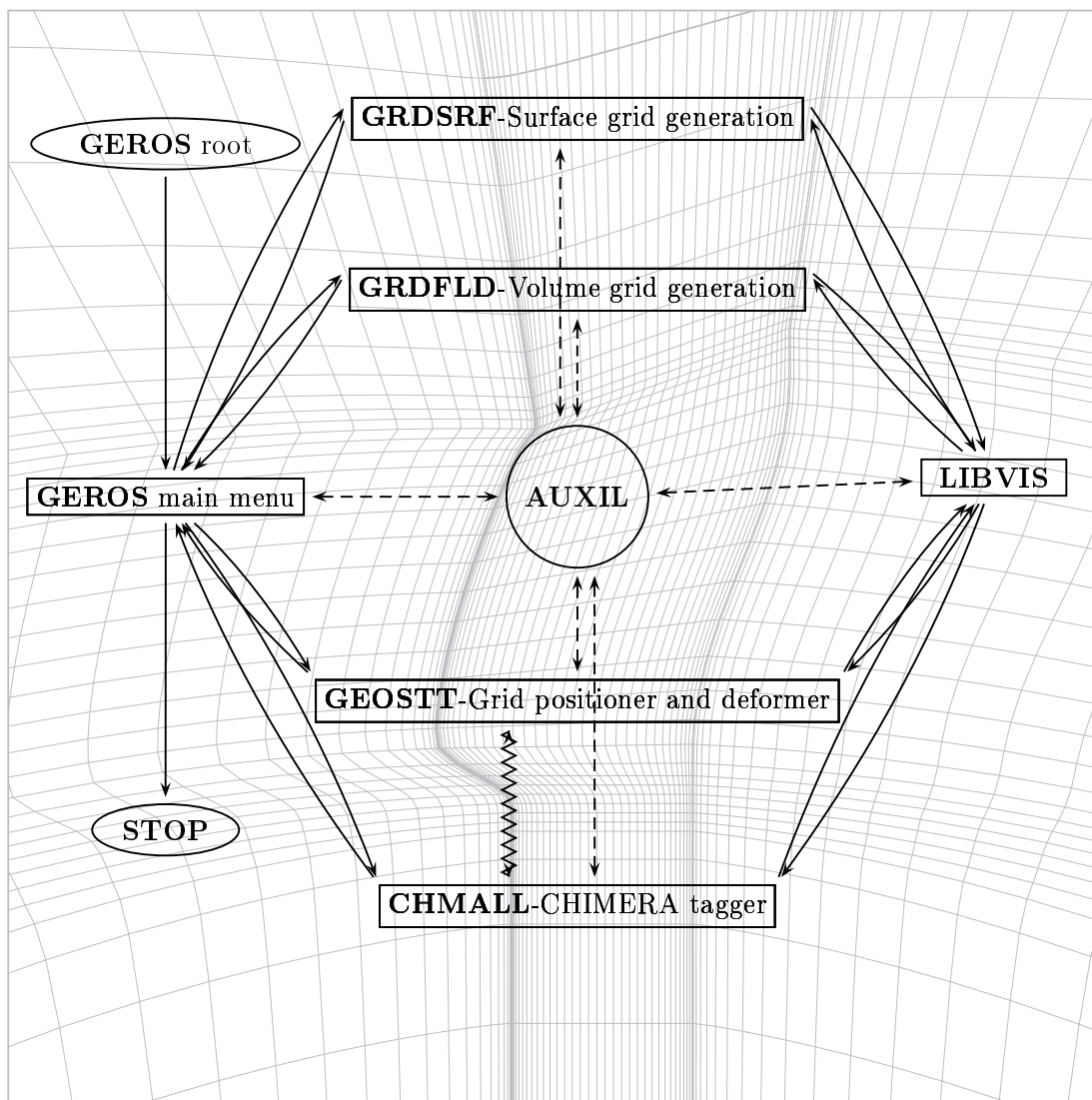


Fig. 1 GEROS structure.

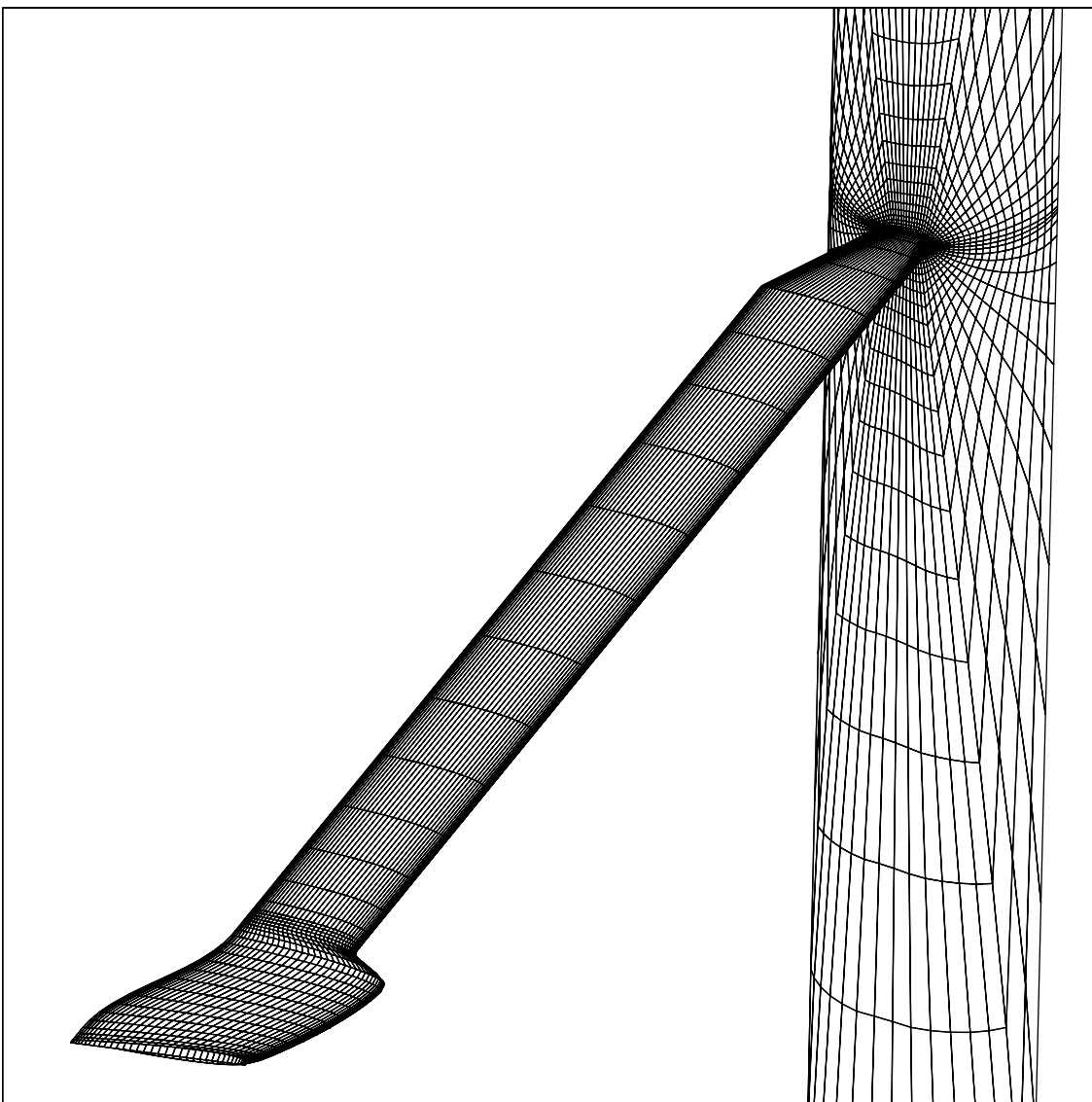


Fig. 2 Surface grid and hub plane grid of BERP blade.

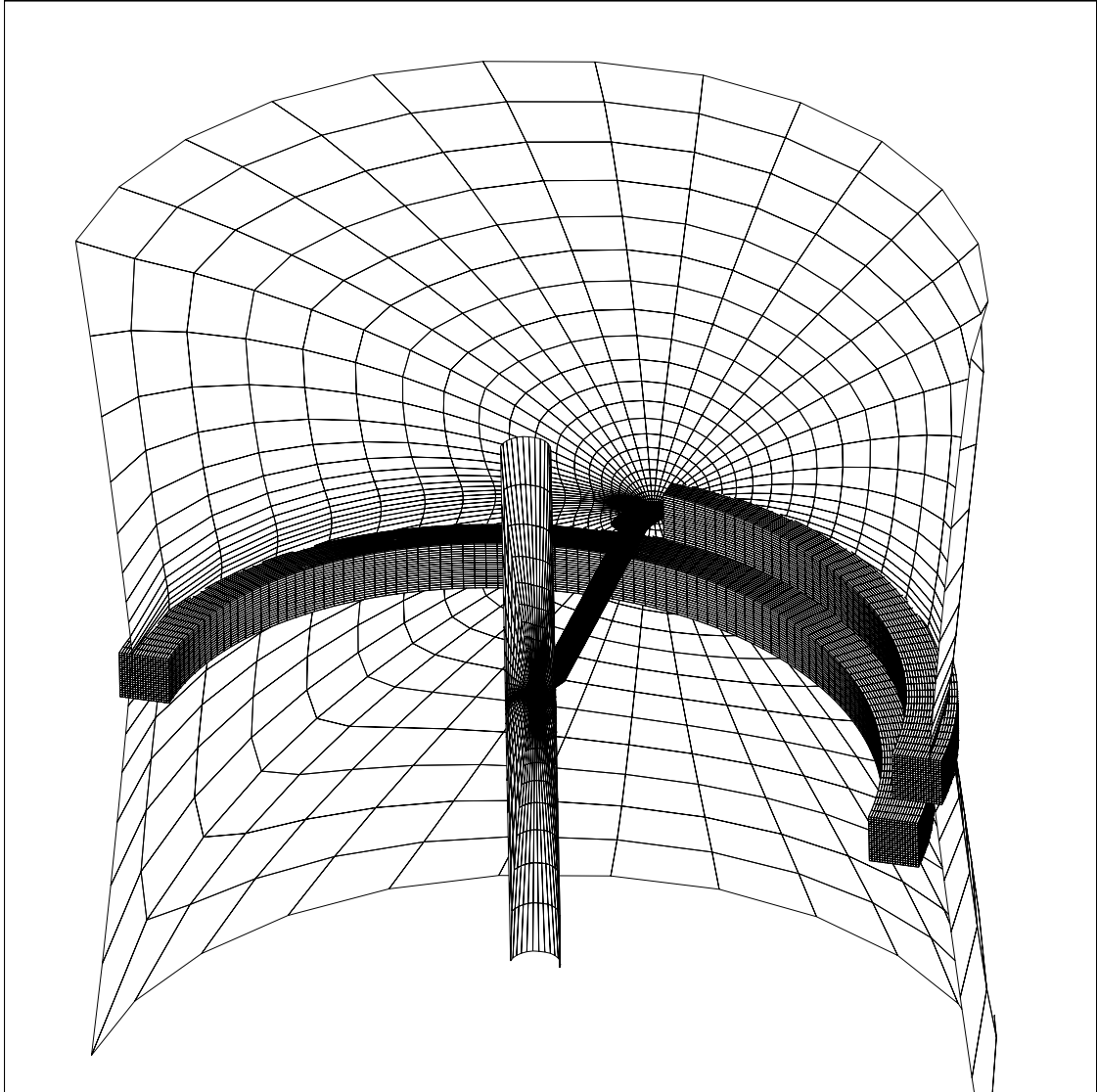


Fig. 3 Characteristic grid planes of BERP blade periodic OH grid, with two embedded HH tip vortex grids.

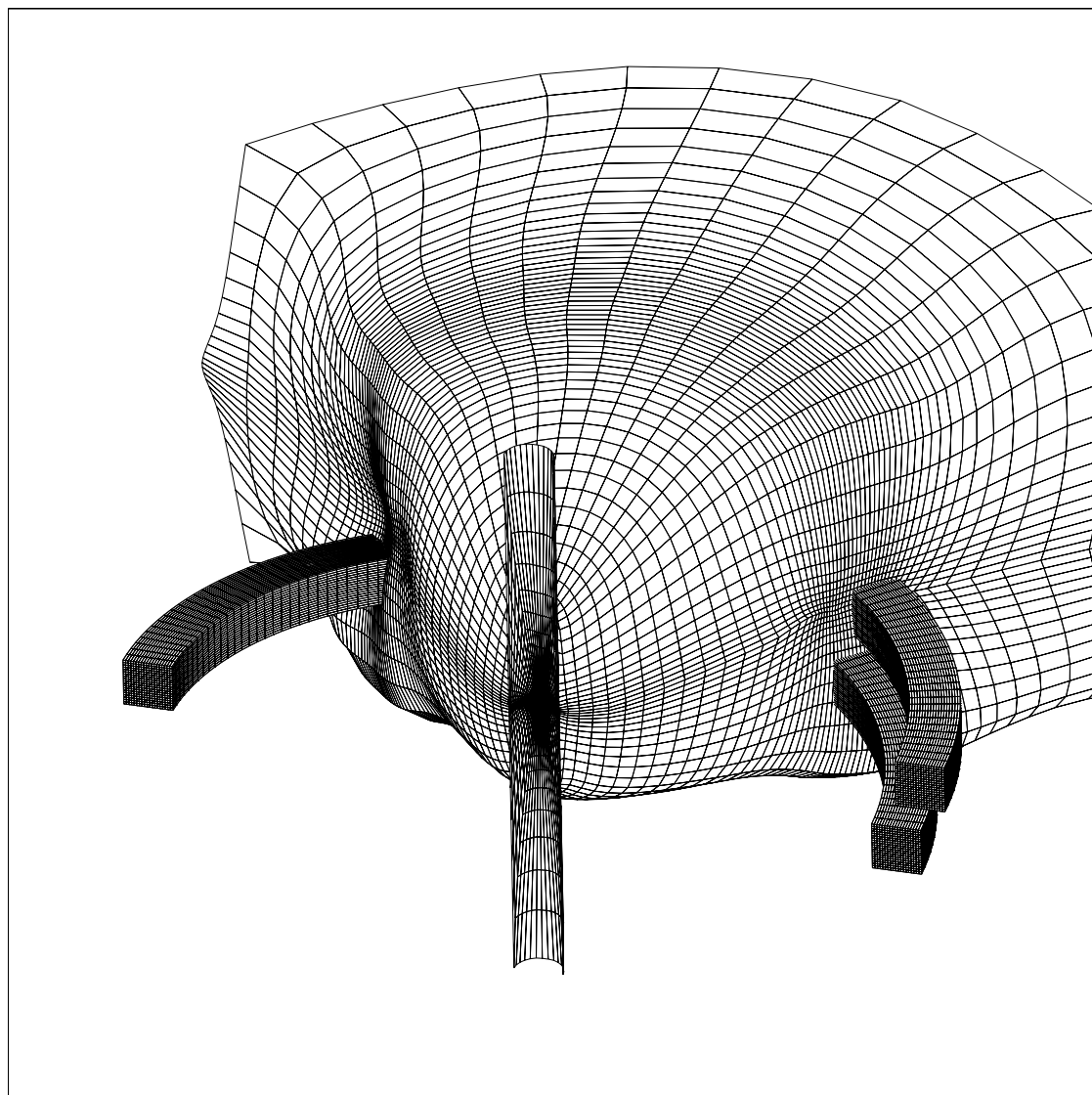


Fig. 4 Characteristic grid planes of BERP blade periodic OH grid, with two embedded HH tip vortex grids.

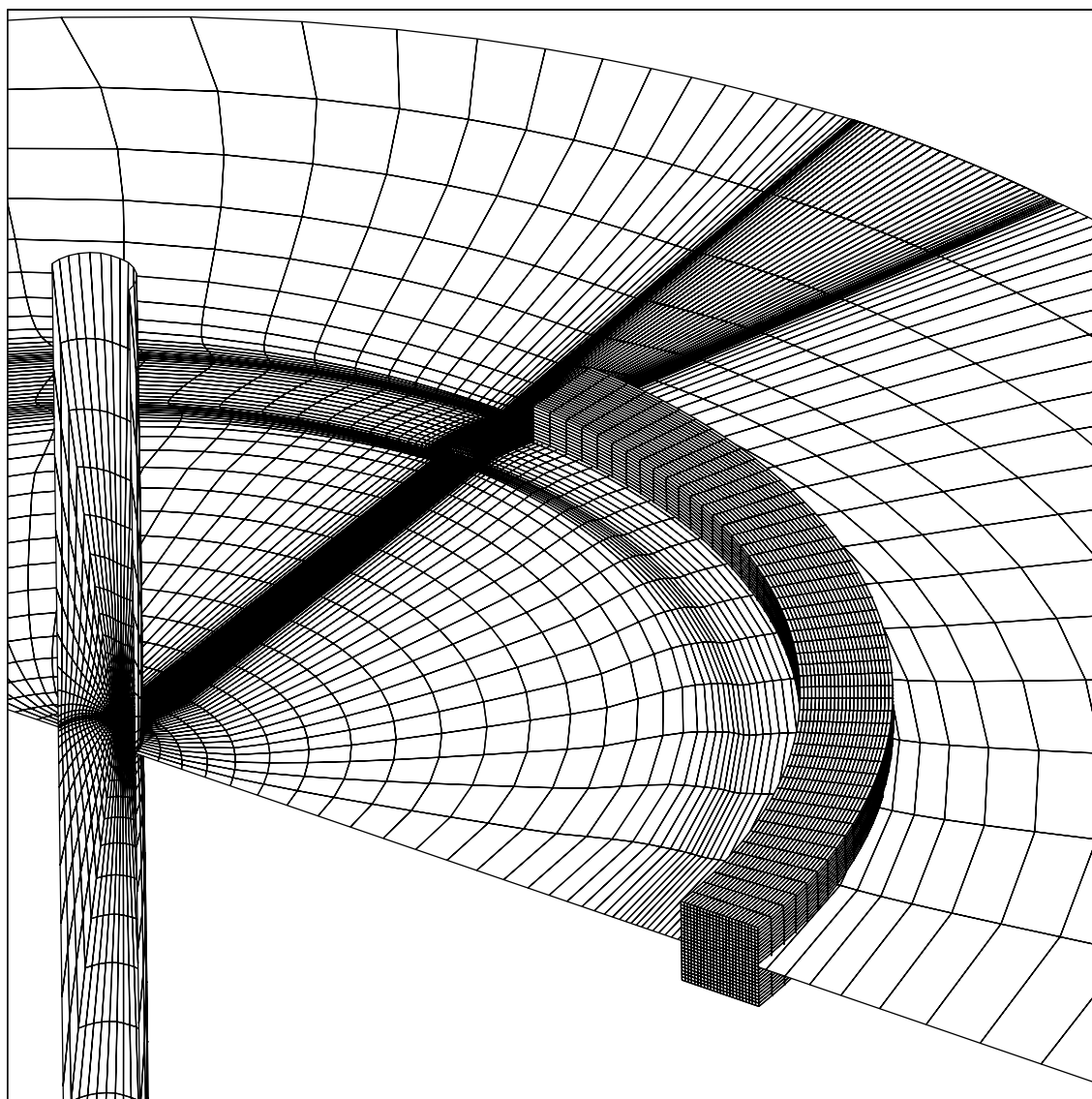


Fig. 5 Tip vortex HH grid and characteristic grid planes of BERP blade OH grid.

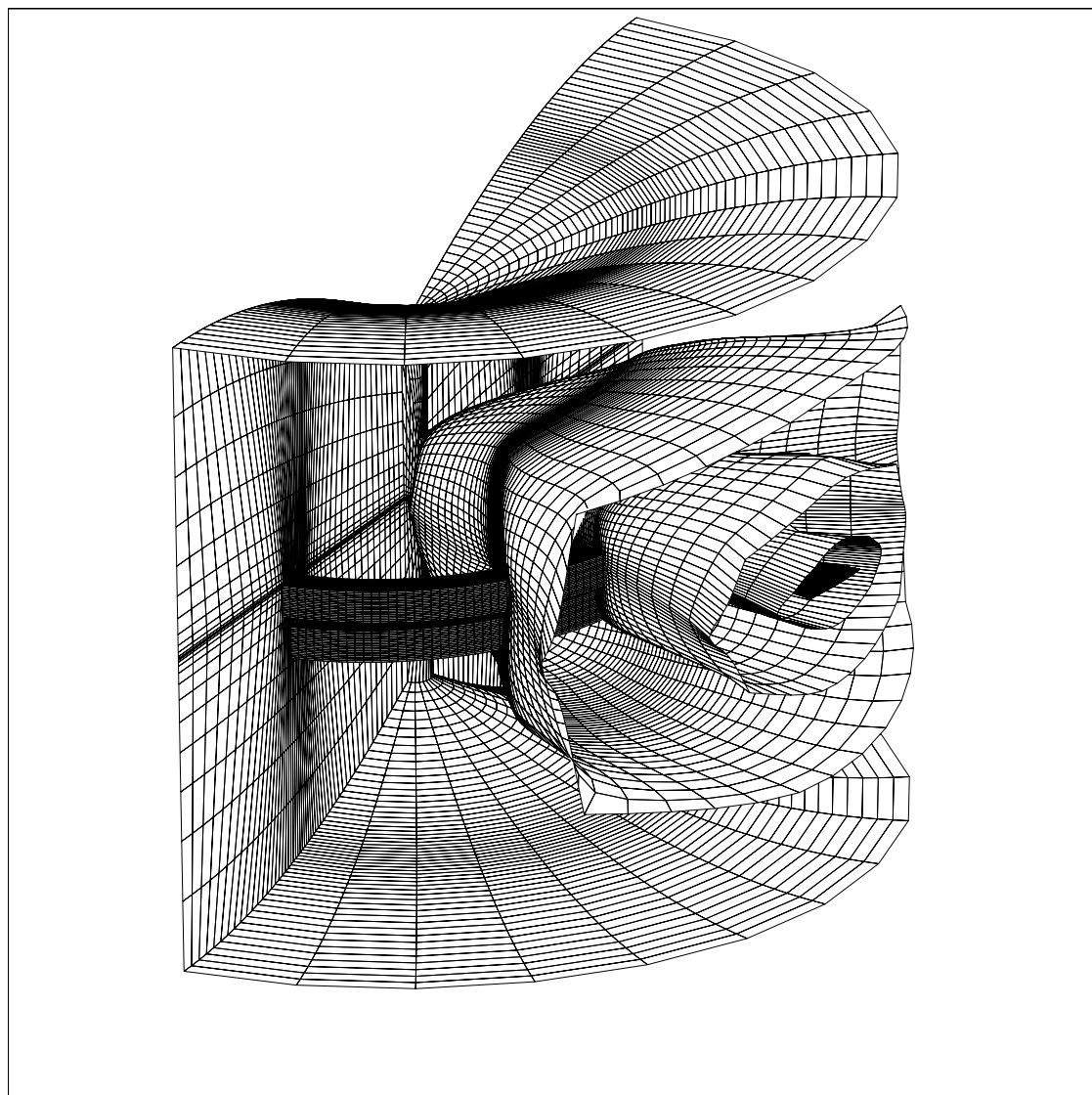


Fig. 6 Characteristic grid planes of BERP blade periodic OH grid, with two embedded HH tip vortex grids.

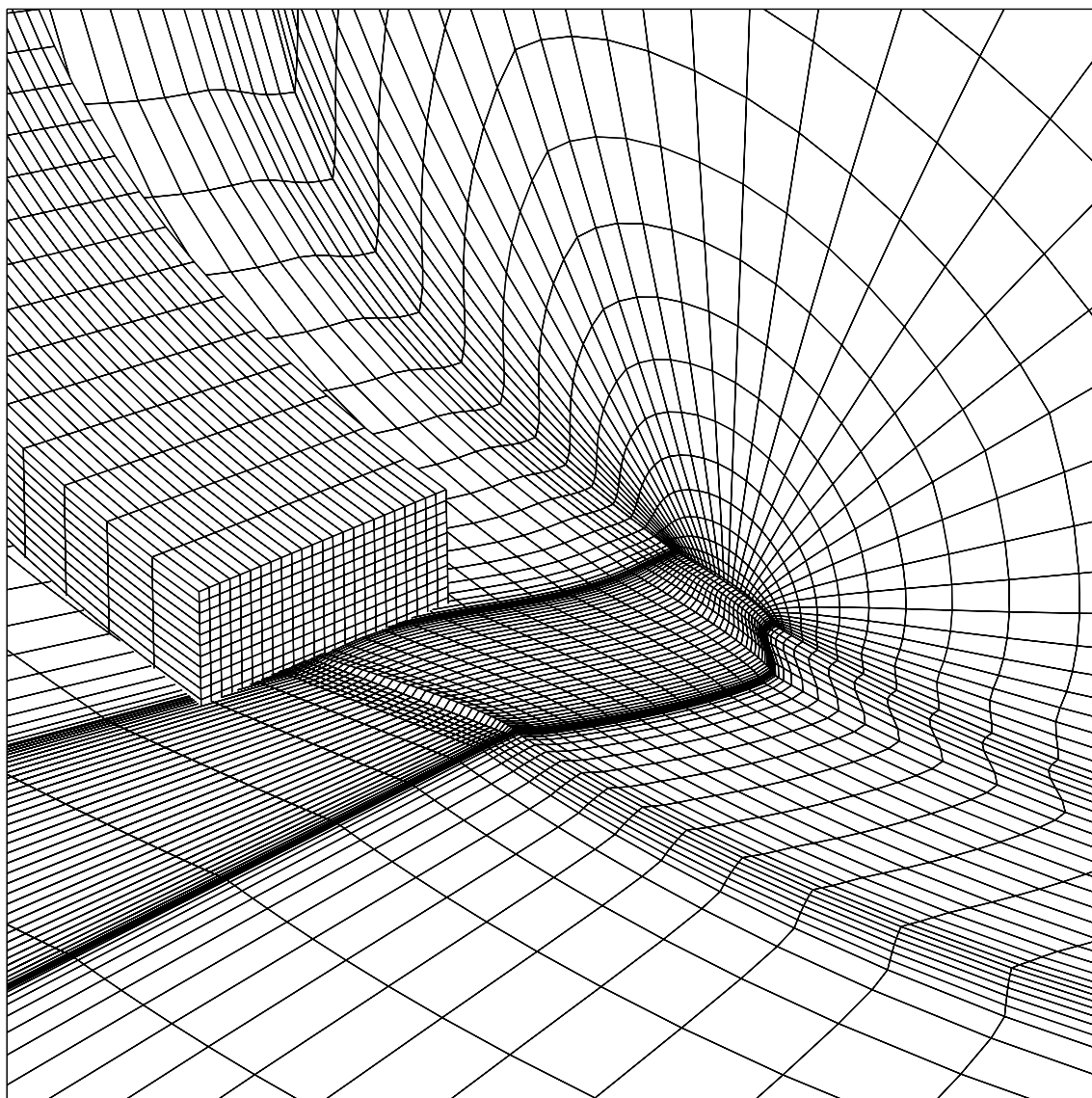


Fig. 7 Tip vortex HH grid and characteristic grid planes of BERP blade OH grid, close-up.

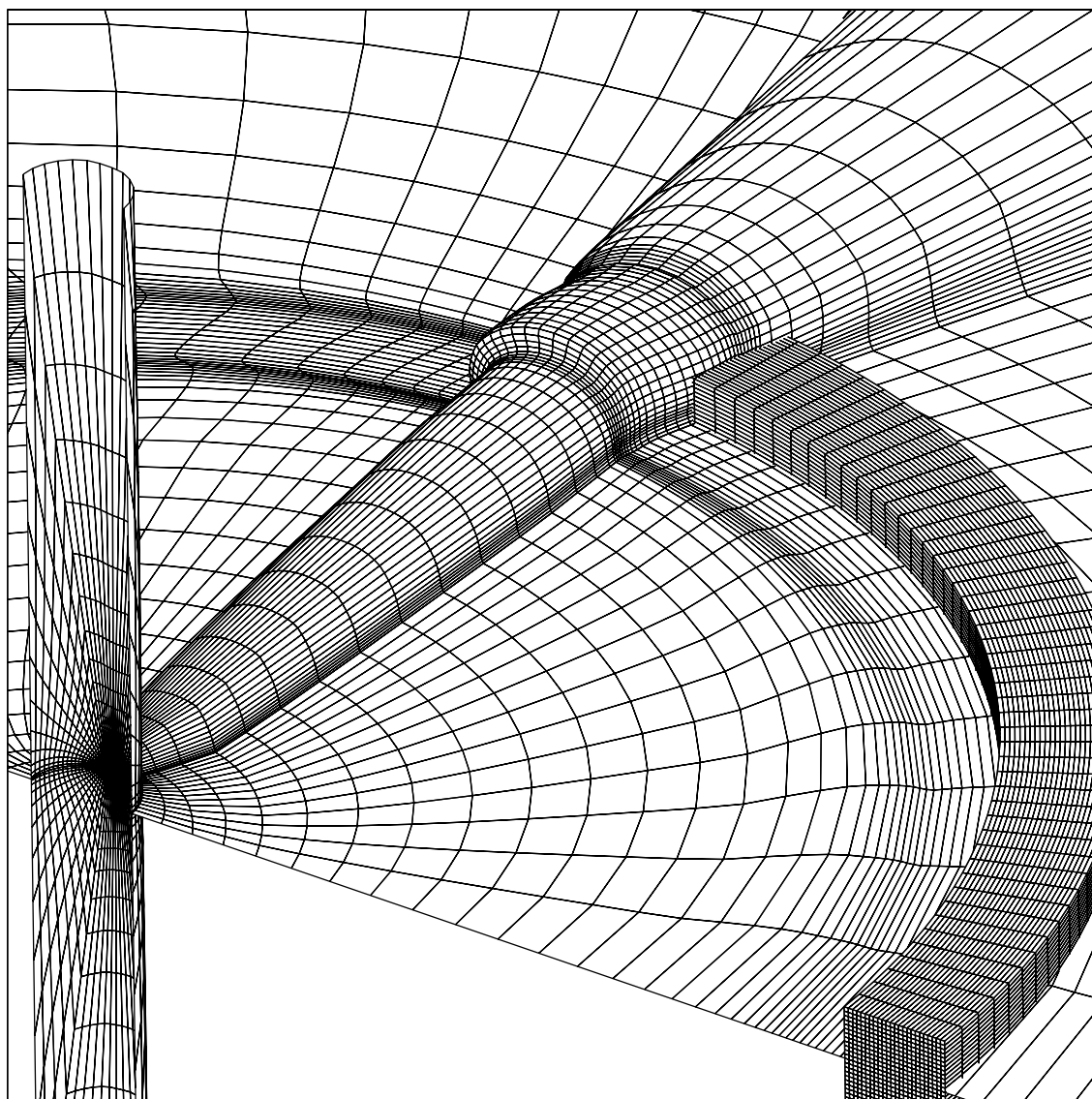


Fig. 8 Tip vortex HH grid and characteristic grid planes of BERP blade OH grid.

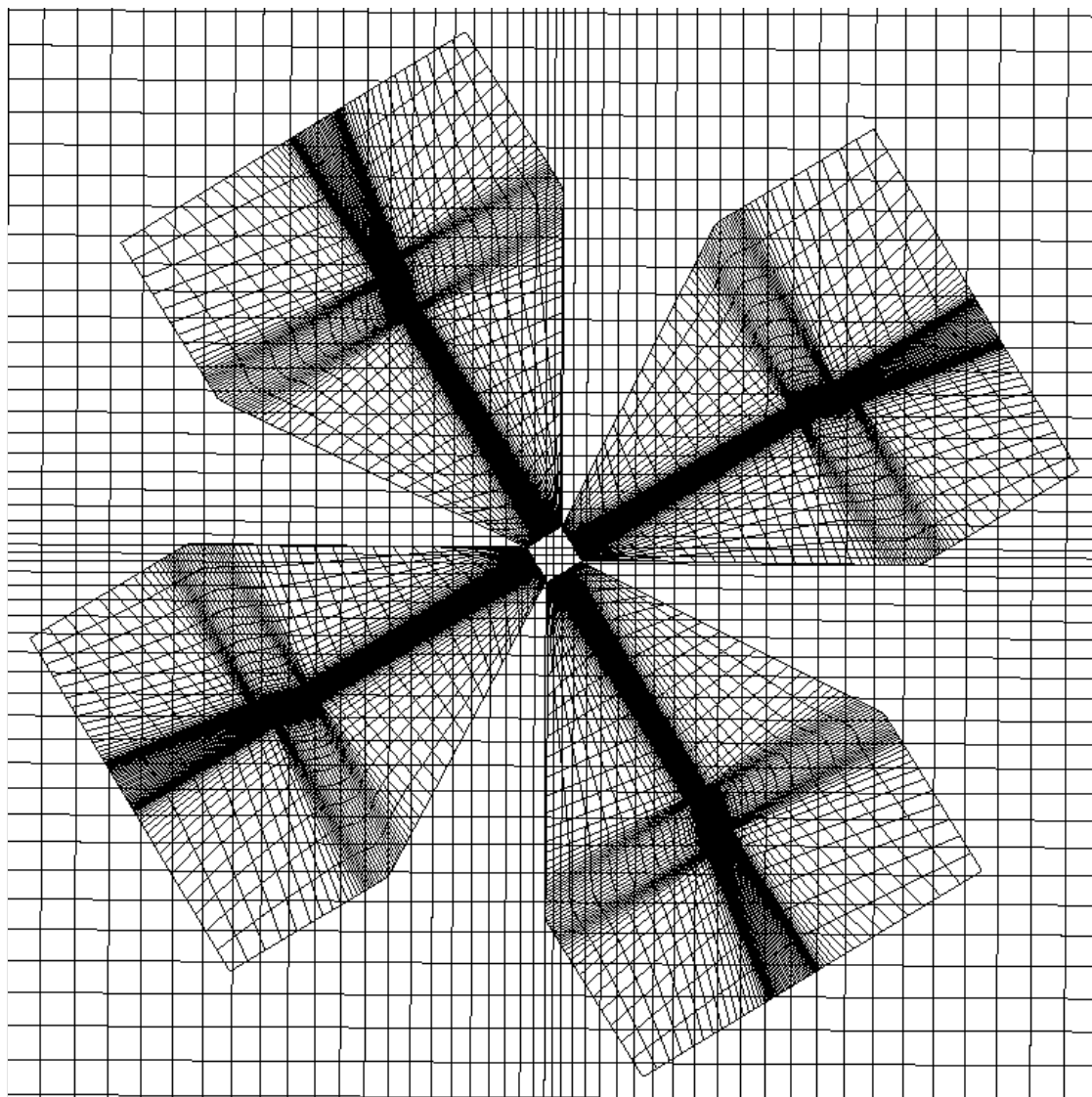


Fig. 9 Typical scenery during the animation of a grid setup (background + OH grid) for a 4-bladed pitching/flapping rotor.

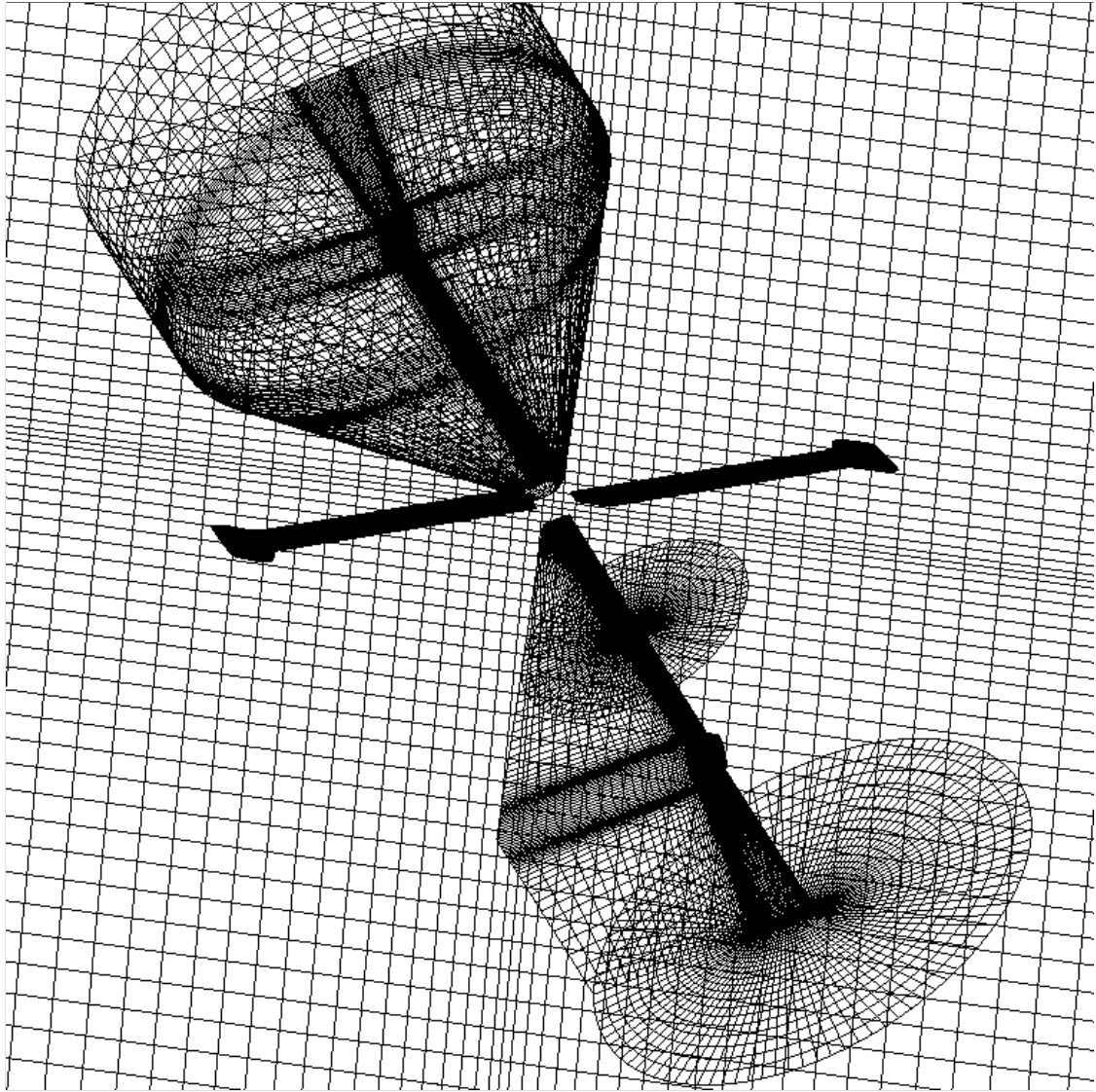


Fig. 10 Typical scenery during the animation of a grid setup (background + OH grid) for a 4-bladed pitching/flapping rotor.

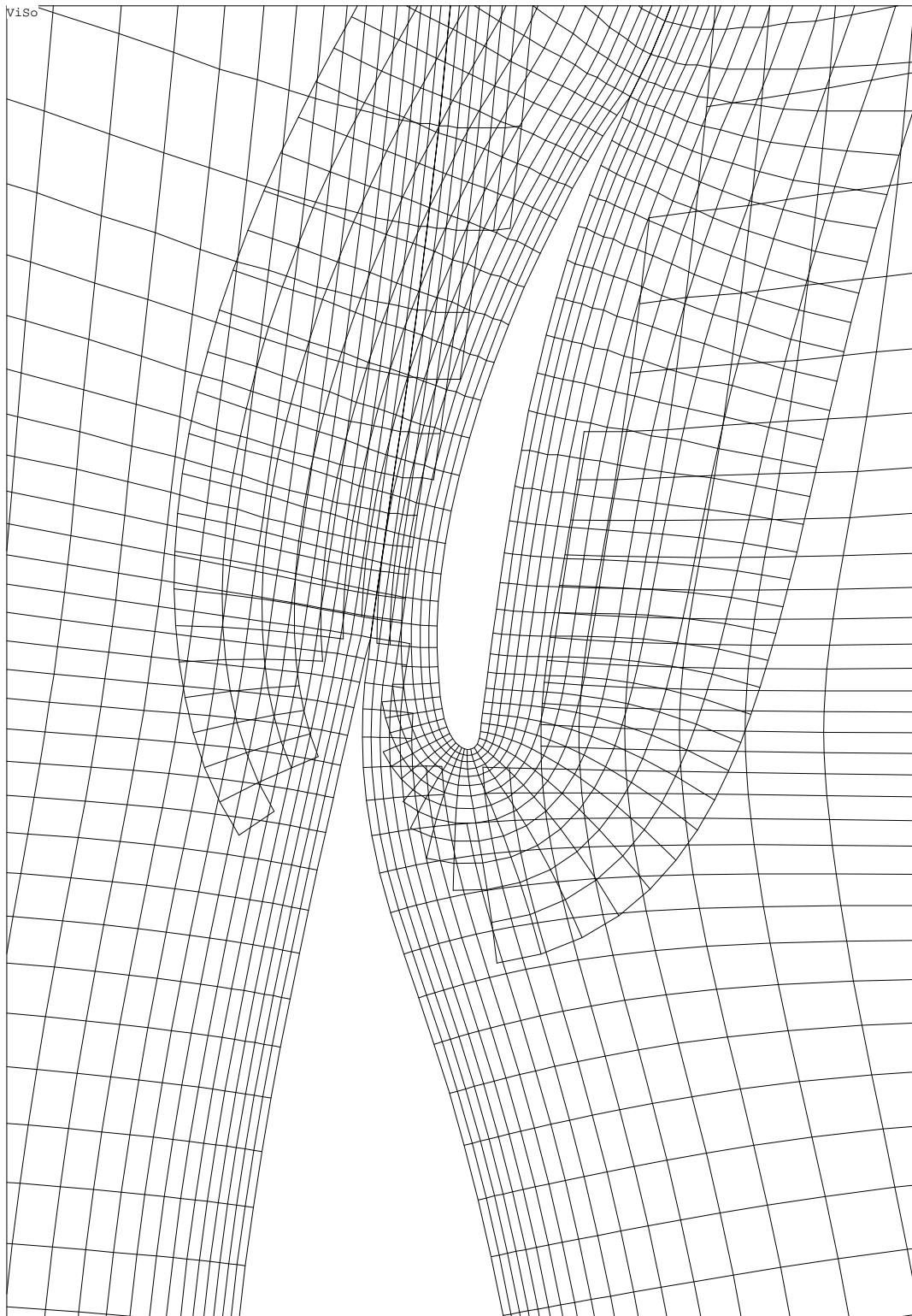


Fig. 11 Results of trivial tagging applied to a 2-component NLR 7301 airfoil, close-up.

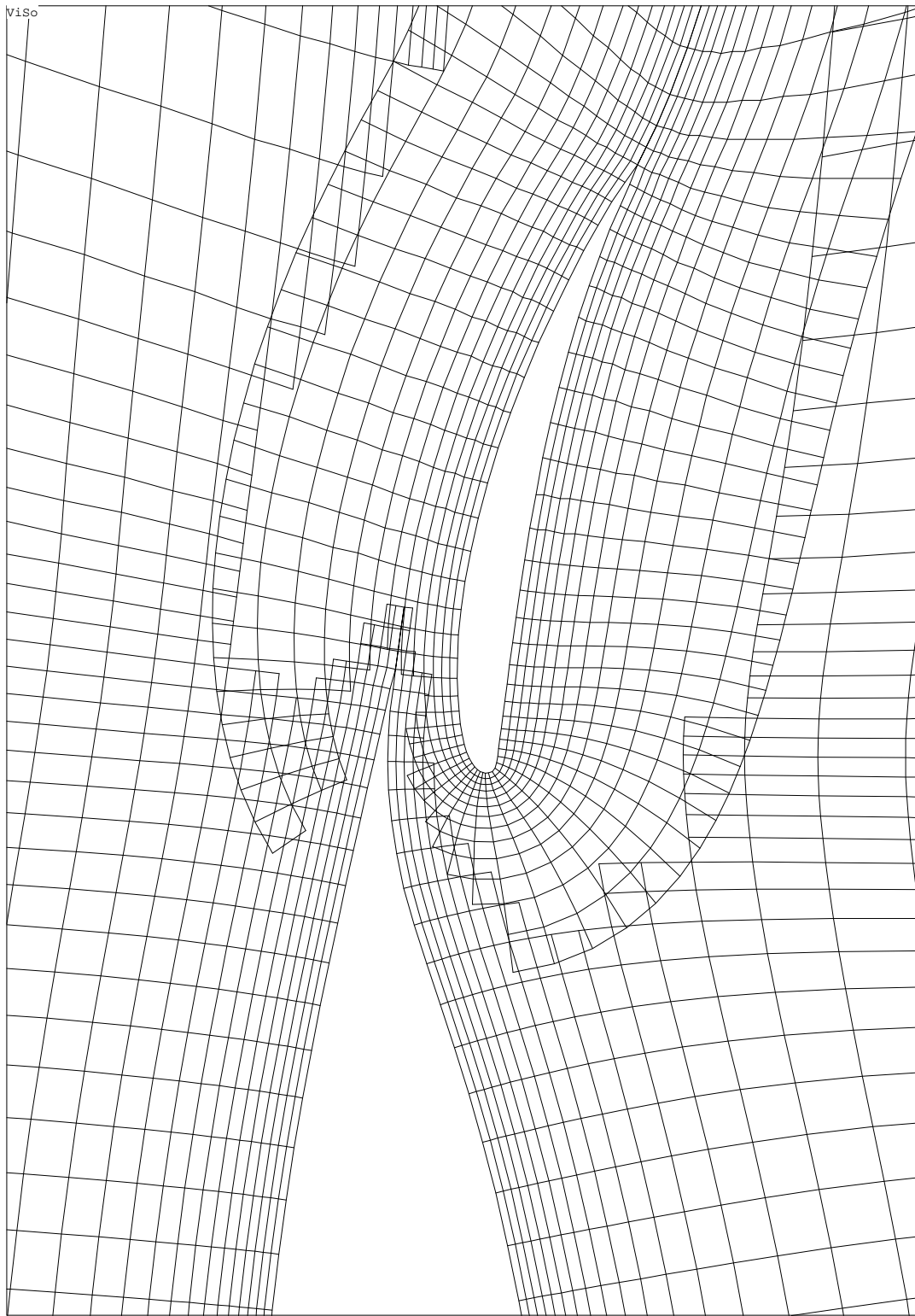


Fig. 12 Results of CPMGRD-like tagging applied to a 2-component NLR 7301 airfoil, close-up.

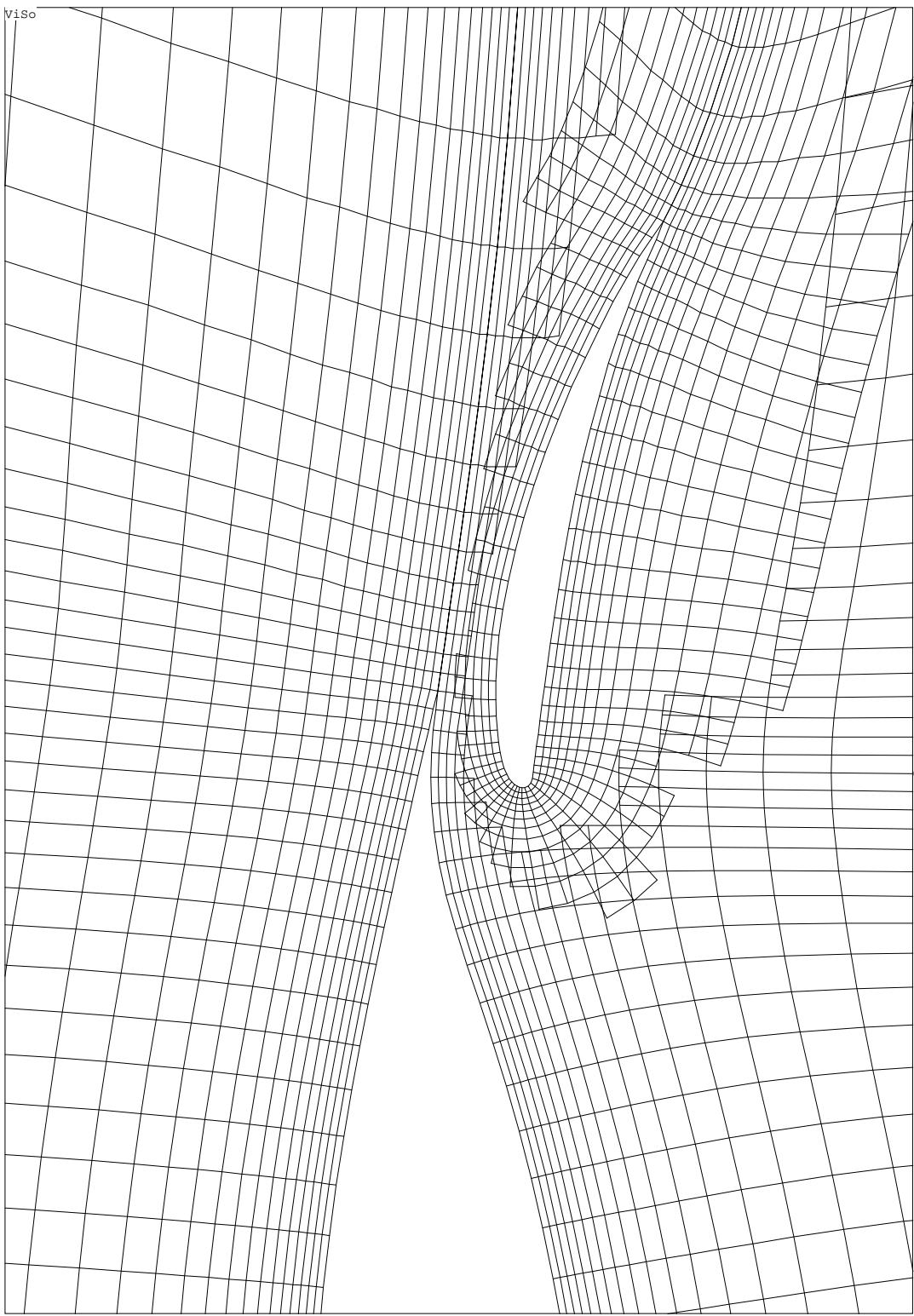


Fig. 13 Results of Smart tagging applied to a 2-component NLR 7301 airfoil, close-up.